British Journal of Pharmacology

DOI:10.1111/j.1476-5381.2011.01380.x
www.brjpharmacol.org

Themed Section: Cannabinoids in Biology and Medicine, Part II

RESEARCH PAPER

Compartmentalization of endocannabinoids into lipid rafts in a microglial cell line devoid of caveolin-1

Neta Rimmerman[1], Heather B Bradshaw[2], Ewa Kozela[3], Rivka Levy[1], Ana Juknat[3] and Zvi Vogel[3]

[1]*Department of Neurobiology, Weizmann Institute of Science, Rehovot, Israel,* [2]*Psychological and brain sciences, Indiana University, Bloomington, IN, USA, and* [3]*Department of Physiology and Pharmacology, Sakler School of Medicine, the Dr Miriam and Sheldon G. Adelson Center for the Biology of Addictive Diseases, Tel Aviv University, Ramat Aviv, Israel*

Correspondence
Neta Rimmerman, Arison Building 302, Department of Neurobiology, Weizmann Institute of Science, Rehovot, 76100, Israel. E-mail: Neta.rimmerman@weizmann.ac.il

Keywords
cannabinoid; endocannabinoid; lipid raft; membrane raft; microglia; Caveolin-1; flotillin-1; cannabidiol; CB_1 receptor; mass spectrometry

Received
5 December 2010
Revised
3 March 2011
Accepted
10 March 2011

BACKGROUND AND PURPOSE

N-acyl ethanolamines (NAEs) and 2-arachidonoyl glycerol (2-AG) are endogenous cannabinoids and along with related lipids are synthesized on demand from membrane phospholipids. Here, we have studied the compartmentalization of NAEs and 2-AG into lipid raft fractions isolated from the caveolin-1-lacking microglial cell line BV-2, following vehicle or cannabidiol (CBD) treatment. Results were compared with those from the caveolin-1-positive F-11 cell line.

EXPERIMENTAL APPROACH

BV-2 cells were incubated with CBD or vehicle. Cells were fractionated using a detergent-free continuous OptiPrep density gradient. Lipids in fractions were quantified using HPLC/MS/MS. Proteins were measured using Western blot.

KEY RESULTS

BV-2 cells were devoid of caveolin-1. Lipid rafts were isolated from BV-2 cells as confirmed by co-localization with flotillin-1 and sphingomyelin. Small amounts of cannabinoid CB_1 receptors were found in lipid raft fractions. After incubation with CBD, levels and distribution in lipid rafts of 2-AG, *N*-arachidonoyl ethanolamine (AEA), and *N*-oleoyl ethanolamine (OEA) were not changed. Conversely, the levels of the saturated *N*-stearoyl ethanolamine (SEA) and *N*-palmitoyl ethanolamine (PEA) were elevated in lipid raft fractions. In whole cells with growth medium, CBD treatment increased AEA and OEA time-dependently, while levels of 2-AG, PEA and SEA did not change.

CONCLUSIONS AND IMPLICATIONS

Whereas levels of 2-AG were not affected by CBD treatment, the distribution and levels of NAEs showed significant changes. Among the NAEs, the degree of acyl chain saturation predicted the compartmentalization after CBD treatment suggesting a shift in cell signalling activity.

LINKED ARTICLES

This article is part of a themed section on Cannabinoids in Biology and Medicine. To view the other articles in this section visit http://dx.doi.org/10.1111/bph.2012.165.issue-8. To view Part I of Cannabinoids in Biology and Medicine visit http://dx.doi.org/10.1111/bph.2011.163.issue-7

Abbreviations

2-AG, 2-arachidonoyl glycerol; ABHD6, α-β-hydrolase domain 6; AEA, *N*-arachidonoyl ethanolamine; CBD, cannabidiol; CB_1, cannabinoid receptor 1; CB_2, cannabinoid receptor 2; NAPE-PLD, *N*-acyl phosphatidylethanolamine phospholipase D; OEA, *N*-oleoyl ethanolamine; PEA, *N*-palmitoyl ethanolamine; PPARα, peroxisome proliferator-activated receptor α; SEA, *N*-stearoyl ethanolamine

Introduction

Membrane rafts are defined as small (10–200 nm), heterogeneous, dynamic, cholesterol and sphingolipid-rich domains. The term membrane raft (interchangeable with lipid raft) is used to convey the importance of both lipids and proteins in membrane raft formation and function (Pike, 2006). Lipid rafts are involved in many functions including intracellular signalling, cellular polarity, molecular sorting, membrane transport and endocytosis (Moffett *et al.*, 2000; Gaus *et al.*, 2003; Chini and Parenti, 2004; Wilson *et al.*, 2004; Lajoie and Nabi, 2010). Caveolae are a subtype of membrane/lipid rafts with electron microscopically visible plasma membrane invaginations. The protein caveolin-1 is a necessary (but not sufficient) component for the formation of caveolae in non-muscle tissues (see Lajoie and Nabi, 2010). Caveolar membrane rafts are involved in lipid molecule endocytosis, transcytosis, transport, trafficking and efflux (Fielding and Fielding, 1995; 1997; Czarny *et al.*, 1999; Sharma *et al.*, 2003; Luo *et al.*, 2010). Other membrane/lipid raft subtypes are less well characterized and include non-caveolar lipid rafts of different types (Lajoie and Nabi, 2010).

Lipid raft/caveolae have been proposed to compartmentalize the endocannabinoid signalling machinery in several cellular systems (Keren and Sarne, 2003; McFarland *et al.*, 2004; 2008 Bari *et al.*, 2005a,b; 2006; 2008; McFarland and Barker, 2005; Sarnataro *et al.*, 2005, 2006; Oddi *et al.*, 2007; Placzek *et al.*, 2008; Rimmerman *et al.*, 2008; Maccarrone *et al.*, 2009). Specifically, several lines of evidence support an association of the cannabinoid CB_1 receptor (nomenclature follows Alexander *et al.*, 2011) with lipid raft/caveolae including: (i) CB_1 receptor C-terminal acylation domain is required for proper interactions with lipid raft-associated G proteins (Mukhopadhyay *et al.*, 1999; Barnett-Norris *et al.*, 2005; Fay *et al.*, 2005; Xie and Chen, 2005); (ii) CB_1 receptor internalization in human embryonic kidney 293 cells-CB_1 transfected cells that occurs via both caveolae and clathrin-coated pits (Keren and Sarne, 2003); (iii) increased CB_1 receptor binding and signalling following cholesterol depletion in C6 glioma cells (Bari *et al.*, 2005a,b; 2006); (iv) CB_1 receptor association with lipid raft fractions/ non-lipid raft fractions in MDA-MB-231 breast cancer cells which depends on receptor activation/ antagonism (Sarnataro *et al.*, 2005; 2006); and (v) CB_1 receptor localization within lipid rafts in human endothelial cells, and CB_1 receptor co-localization with caveolin-1 in C6 glioma cells (Bari *et al.*, 2006; 2008).

N-arachidonoyl glycerol (2-AG) and *N*-arachidonoyl ethanolamine (AEA), two major endocannabinoids that interact with CB_1 and CB_2 receptors have been characterized in lipid rafts (Rimmerman *et al.*, 2008). We previously investigated their compartmentalization in caveolin-1-expressing F-11 cells (a dorsal root ganglion-like cell line). We showed that membrane/lipid rafts (rich in caveolin-1, flotillin-1 and lipid markers) compartmentalize the biochemical machinery for the production of 2-AG that includes the 2-AG precursor arachidonoyl-containing diacyl glycerol, and the synthetic enzyme diacyl glycerol lipase α (DGLα; Rimmerman *et al.*, 2008). Additionally, endogenous AEA and one of its biosynthetic enzymes, *N*-acyl phosphatidylethanolamine phospholipase D (NAPE-PLD) were found in lipid raft as well as in non-raft fractions (Rimmerman *et al.*, 2008). A similar trend was observed following incubation with exogenous deuterium labelled AEA [($^2H_8$)-AEA]. On the other hand, deuterium labelled arachidonic acid, a direct metabolite of [$^2H_8$]-AEA, was localized mostly to non-lipid raft fractions consistent with the theory of caveolar-mediated endocytosis of AEA (McFarland *et al.*, 2004; McFarland and Barker, 2005).

AEA belongs to a larger family of *N*-acyl ethanolamines (NAE) such as the monounsaturated [(18:1)-containing acyl chain] *N*-oleoyl ethanolamine (OEA), and the saturated [(18:0) and (16:0)-containing acyl chain], *N*-stearoyl ethanolamine (SEA) and *N*-palmitoyl ethanolamine (PEA) respectively. NAEs were shown to increase during brain disease, and to produce anti-inflammatory effects through different mechanisms (see Franklin *et al.*, 2003; Hansen, 2010). OEA was shown to interact with the nuclear receptor peroxisome proliferator-activated receptor α (PPARα) and the orphan G protein coupled receptor, GPR119. PEA was shown to interact with PPARα, GPR119 and GPR55 (Fu *et al.*, 2005; Lo Verme *et al.*, 2005a,b; Overton *et al.*, 2006, 2008; O'Sullivan *et al.*, 2007; Godlewski *et al.*, 2009). SEA interacts with a yet unidentified target to modulate cellular signalling (Maccarrone *et al.*, 2002; Hansen, 2010). The compartmentalization of OEA and SEA in lipid rafts has not yet been investigated.

The mechanisms leading to 2-AG and NAE metabolism differ between cell types, reflecting differential expression of gene products, enzymes, lipid membrane composition and trafficking mechanisms. In this study, we characterize the membrane compartmentalization of 2-AG and NAEs into lipid rafts in the BV-2 microglial cell line, which we found to be devoid of caveolin-1. BV-2 microglial cells express CB_1 and CB_2 receptors, the lysophosphatidylinositol/cannabinoid receptor GPR55 and the putative abnormal-cannabidiol receptor GPR18 (Pietr *et al.*, 2009; McHugh *et al.*, 2010; Stella, 2010). In addition, they express the enzyme α-β-hydrolase domain 6 (ABHD6) that controls the accumulation of 2-AG and the efficacy of this compound at cannabinoid receptors (Marrs *et al.*, 2010). Furthermore, PEA was shown to be metabolized via a URB602-sensitive enzyme of yet unknown identity, and AEA through fatty acid amide hydrolase (FAAH) in BV-2 cells (Muccioli *et al.*, 2007; Muccioli and Stella, 2008).

Our group recently reported that the non-psychoactive plant cannabinoid, cannabidiol (CBD) inhibits pro-inflammatory pathways in lipopolysaccharide-activated BV-2 cells (Kozela *et al.*, 2010). In addition, our gene array analysis studies indicate that CBD exerts immunosuppressive effects by regulating stress response genes (Juknat *et al.*, 2012). Here, we compared the compartmentalization of 2-AG and NAEs in lipid raft fractions, as well as their levels in whole cells with growth medium, between vehicle and CBD-treated cells. We show that BV-2 cells do not express caveolin-1 mRNA or protein, and thus, are devoid of the caveolar-membrane/lipid raft subtype. The compartmentalization of 2-AG in these cells was generally similar to F-11 cells (which express caveolin-1); however, while the membrane/lipid rafts in F-11 cells were well separated from the non-raft fractions by their density profile (Rimmerman *et al.*, 2008), BV-2 lipid rafts and non-lipid raft fractions showed a much closer density. The CB_1 receptor is localized mostly to non- lipid raft fractions with small amounts present in lipid raft fractions. In addition, we show that following CBD treatment, the levels of 2-AG were not affected in membrane/lipid raft fractions or whole cells

with growth medium. The levels of AEA and OEA increased significantly in whole cells with growth medium, while the levels of PEA and SEA increased significantly in membrane/lipid rafts fractions.

Methods

Cell culture

The BV-2 murine microglial cell line, originally generated by E. Blasi (University of Perugia, Perugia, Italy; Blasi *et al.*, 1990), was kindly provided by Prof E.J. Choi from the Korea University (Seoul, Korea). Cells were grown under 5% CO_2 at 37°C in Dulbecco's modified Eagle's medium containing high glucose (Gibco-BRL, Gaithersburg, MD, USA) supplemented with 5% heat-inactivated foetal bovine serum, streptomycin (100 μg·mL^{-1}) and penicillin (100 U·mL^{-1}) (Biological Industries Ltd, Kibbutz Beit Haemek, Israel). Cells were used up to passage 25.

Lipid analysis from whole BV-2 cells and media

BV-2 cells were grown for 24 h on 10 cm plates in growth medium. Media was replaced with 5 mL fresh growth medium 1 h before treatment. BV-2 cells were then treated with either vehicle (ethanol 0.1%) or CBD (10 μM). Cells together with media were scraped into 7 mL 100% HPLC-grade methanol. Whole cells with growth medium were collected from independent plates at four time points (10, 30, 60 and 210 min; n = 3 per condition; except for vehicle at 210 min, n = 2). The solution was then vortexed and centrifuged at 200× g for 5 min. Internal standards were added to supernatant samples and HPLC-grade water was added to make a 75% aqueous solution. Lipids were then extracted as previously described (Bradshaw *et al.*, 2006). Briefly, 500 mg C8 Bond Elut solid phase extraction columns (Varian, Harbor city, CA, USA) were conditioned with 5 mL HPLC-grade methanol followed by 3.0 mL HPLC-grade water. The 75% aqueous solutions were loaded onto separate columns, which were then washed with 3 mL water. Two sequential elutions (1.5 mL 50%, and 2 mL 100% methanol) were collected for mass spectrometric analysis. Samples were dried down by speed vac and reconstituted in 400 μL 100% HPLC-grade methanol for lipid analysis.

Membrane fractionation

Procedures for fractionation were adapted from the method of Macdonald and Pike (2005). Cells were plated 24 h before the experiment. On the day of the experiment, cells from four 150 mm plates for each experimental condition were washed once with PBS and scraped into a total of 25 mL of 4°C base buffer (20 mM Tris-HCl, 250 mM sucrose, pH 7.8) containing 1 mM calcium chloride and 1 mM magnesium chloride. Cells were centrifuged in a polystyrene tube at 200× g for 7 min at 4°C. The pellet was re-suspended in 1.0 mL of base buffer containing calcium and magnesium, and protease inhibitors were added (1 mM phenylmethylsulphonyl fluoride, 20 μg·mL^{-1} leupeptin, 1 μg·mL^{-1} aprotinin and 2 μM pepstatin). Cells were then lysed by passage through a 27 g × 3″ needle, 20 times, and centrifuged at 1000× g for 10 min at 4°C. The post-nuclear supernatant was transferred to a new tube, the pellet was re-suspended in base buffer containing calcium chloride, magnesium chloride and protease inhibitors, and the procedure was repeated. The 2 mL post-nuclear supernatants were combined and 50% OptiPrep (Axis Shield, Dundee, UK) in base buffer was added to give a 4 mL solution of 25% OptiPrep. An 8 mL continuous density gradient of 20%–0% OptiPrep in base buffer was formed on top of the 4 mL 25% OptiPrep solution in Ultra-Clear™ (14 × 89 mm) centrifuge tubes. The gradient was centrifuged using an SW-41 swinging bucket rotor (Beckman Coulter, Fullerton, CA, USA) for 90 min at 52 000× g at 4°C. 16 fractions of 0.75 mL were collected from each gradient.

To confirm our results, we used a second fractionation method according to Ostrom *et al.* (2001) which was modified from the original method of Song *et al.* (1996). Briefly, cells were scraped into 500 mM sodium bicarbonate, pH 11 (including protease inhibitors). Cells were then homogenized 10 times with a Dounce homogenizer, then were polytroned 10 s × 3 times, and sonicated 20 s × 3 times. The 2 mL homogenate was mixed with 2 mL of 90% sucrose (containing MES 25 mM, and NaCl 150 mM) to a final concentration of 45% sucrose. The 4 mL homogenate was placed in the bottom of an Ultra-Clear™ (14 × 89 mm) centrifuge tube. On top of the homogenate were placed 4 mL 35% sucrose (containing MES 25 mM, NaCl 150 mM, Na_2CO_3 250 mM), and 4 mL of 5% sucrose in the same buffer to form a discontinuous gradient. The gradient was centrifuged using an SW-41 swinging bucket rotor for 20 h at 160 000× g at 4°C. Eleven fractions of 1 mL were collected from each gradient.

Mass spectrometric analysis of lipids in fractions

For lipid analysis, 0.6 mL of each fraction was removed and 2 mL of HPLC-grade methanol were added. [$^2H_8$]-AEA (200 pmol) was added to each sample and diluted with HPLC-grade water to make a 75% aqueous solution. Lipids were extracted as previously described (Bradshaw *et al.*, 2006). Briefly, 500 mg C8 Bond Elut solid phase extraction columns (Varian) were conditioned with 5 mL HPLC-grade methanol, followed by 3.0 mL HPLC water. The 75% aqueous solutions containing the fractions were loaded onto separate columns, which were then washed with 20 mL water. Five sequential elutions (1.5 mL each of 30, 50, 85 and 100% methanol) were collected for mass spectrometric analysis. As described previously (Bradshaw *et al.*, 2006), sample analysis of lipids was carried out as follows. An aliquot of each of the eluates was loaded using a Shimadzu SCL10Avp (Wilmington, DE, USA) or an LC Packings Ultimate-3000 (Sunnyvale, CA, USA) autosampler onto a reversed phase Zorbax 2.1 × 50 mm C8 column maintained at 40°C. HPLC gradient formation at a flow rate of 200 μL·min^{-1} was achieved by a system comprised of a Shimadzu controller and two Shimadzu LC10ADvp pumps or an LC Packings controller and an LPG-3000 loading pump. Lipid levels in the samples were analysed in multiple reaction monitoring (MRM) mode on a triple quadrupole mass spectrometer, using either the API 3000 or the API 4000 (Applied Biosystems/MDS SCIEX, Foster city, CA, USA), with electrospray ionization. Methods for lipid analysis were created and optimized by flow injection of lipid standards. All calculations for quantitation experiments were based on cali-

bration curves using synthetic standards. The following molecular ion and fragment ion pairs were used to quantify lipids in MRM mode: (18:0)-sphingomyelin 731.7/184.1; 2-AG 379.3/287.3; AEA 348.2/62.1; PEA 300.2/62.1; SEA 328.2/62.1; OEA 326.2/62.1; CBD 315.2/193.1.

Western blot analysis

Membrane components present in gradient fractions were lysed by the addition of sodium dodecyl sulphate (SDS) (Sigma-Aldrich), NP-40 (EMD Biosciences Inc., La Jolla, CA, USA) and Triton X-100 (Sigma-Aldrich) to a final concentration of 0.5, 1 and 1% respectively. Samples were incubated on ice for 30 min. Laemmli Loading buffer was added to the samples and they were denatured for 3 min at 70°C using a hot water bath. Aliquots of 20 μL from each sample were separated by an 8% or 10% SDS-polyacrylamide gel electrophoresis and transferred to nitrocellulose membranes. The membranes were blocked in blocking buffer consisting of TBST [10 mM Tris-HCl (pH 7.5), 150 mM NaCl and 0.1% Tween-20] with 5% w/v skim milk. The membranes were washed five times with TBST and incubated overnight at 4°C in the presence of primary antibody or antibody + blocking peptide in 3% BSA. The following affinity-purified antibodies were used for the Western blot analyses: anti-flotillin-1 (1:500 dilution), anti-caveolin-1 (1:500 dilution), anti-transient receptor potential channel V2 (TRPV2; 1:500 dilution), anti-CB_2 receptor (1:500 dilution), anti-CB_1 receptor (1: 500 dilution), anti- β-actin (1:1000–2000 dilution) and anti-lysosomal-associated membrane protein 1 (LAMP1) (1: 1000 dilution). The membranes were washed five times with TBST, and then incubated for 45–60 min with either HRP-goat anti-rabbit IgG, HRP-goat anti-mouse IgG (1:10 000 dilution) or HRP-rat anti-mouse IgG (1:10 000) in 5% milk (or 3% BSA for the CB_1 receptor primary antibody). The blots were washed five times and processed using chemiluminescent detection. The detection of CB_1 receptors needed a much longer film exposure compared with CB_2 receptors, due to lower levels of the CB_1 receptor protein.

Isolation of total RNA, reverse transcription and real-time quantitative PCR (qPCR)

Primers for mouse caveolin-1 (NM_007616.3) and for mouse caveolin-2 (NM_016900.3) were designed as *assay on demand* by Qiagen (Hilden, Germany). The following primers were used for mouse caveolin-1, forward AGCTCACATTACAGC TCTGCCCTT, reverse AGTGTCGGCAAGACTGAAGGAGAA; for caveolin-2, forward TTGCGGGTATCCTGTTTGCT, reverse AGTTGCATGCTGACCGATGA; and for mouse β-microglobulin, forward ATGGGAAGCCGAACATACTG, reverse CAGTCTCAGTGGGGGTGAAT. RNA was extracted using the Versagene RNA purification kit (Gentra, Minneapolis, MN, USA), and RNA samples (2 μg) were reverse transcribed using the QuantiTect Reverse Transcription Kit from Qiagen including DNase treatment of contaminating genomic DNA. Expression of caveolin-1 and caveolin-2 mRNAs were determined by qPCR, using β-microglobulin as a normalizing gene, as previously described (Butovsky *et al.*, 2006). Normal and mock reversed transcribed samples (in the absence of reverse transcriptase), as well as no template controls (total mix without cDNA), were run for each of the examined mRNA's. qPCR reactions were subjected to an initial step of 15 min at 95°C to activate the HotStar Taq DNA polymerase, followed by 40 cycles consisting of 15 s at 94°C, 30 s at 60°C and 30 s at 72°C. Fluorescence was measured at the end of each elongation step. Data were analysed using the Rotor-Gene software (Corbett Life Sciences, Mortlake, Australia) and a threshold cycle value C_t was calculated from the exponential phase of each PCR sample. Amounts of mRNAs were calculated and expressed in relative units of SYBR Green fluorescence.

Data analysis

Data are shown as means ± SEM. Differences in lipid levels were assessed by one-way analysis of variance (ANOVA) with Fisher's least significant difference (LSD) *post hoc* test or Bonferroni *post hoc* test (SPSS, Chicago, IL, USA), as specified in the Figure legends. Differences were considered significant for $P < 0.05$.

Materials

[$^2H_8$]-*N*-arachidonoyl ethanolamine [($^2H_8$)-AEA], AEA, PEA, SEA and 2-AG were purchased from Cayman Chemical (Ann Arbor, MI, USA). CBD was received from NIDA. Sphingomyelin standards were purchased from Avanti Polar Lipids, Inc (Alabaster, AL, USA). High-performance liquid chromatography (HPLC) grade methanol, acetonitrile and isopropyl alcohol were purchased from VWR international (Plainview, NY, USA) and HPLC-grade water was obtained using a MilliQ Gradient apparatus from Millipore (Milford, MA, USA). HPLC-grade acetic acid and ammonium acetate were purchased from Sigma-Aldrich (St. Louis, MO, USA).

The affinity purified rabbit polyclonal antibodies L15-CB_1, and CT_t-CB_2 were provided by Dr Ken Mackie, Bloomington, IN, USA and used with their respective blocking peptides. The TRPV2 rabbit polyclonal antibody (ACC-039) targeting an extracellular epitope was purchased from Alomone (Jerusalem, Israel) and was used with the supplied blocking peptide. Mouse monoclonal antibody for caveolin-1 (C37120), and mouse flotillin-1 (312–428) were purchased from BD Transduction Laboratories (San Diego, CA, USA). Mouse monoclonal antibody against β-actin was purchased from Santa Cruz Biotechnology (Santa Cruz, CA, USA), and rat monoclonal anti-LAMP-1 (1D4B) was purchased from Developmental studies hybridoma bank (NIH).

Results

Localization of lipid raft markers

BV-2 cells were fractionated using a continuous (0–20% OptiPrep), detergent-free, density gradient (Macdonald and Pike, 2005). The distribution of the lipid raft marker [18:0]-sphingomyelin in BV-2 cells (Figure 1A) was equivalent to the distribution of the membrane/lipid rafts protein marker flotillin-1 (Figure 1B). Note that the lipid rafts isolated from BV-2 cells (fractions 7–10) are distributed differently on the continuous OptiPrep density gradient when compared with lipid rafts isolated from F-11 cells (fractions 10–13; Rimmerman *et al.*, 2008). In the BV-2 cells fraction 6 represents an interface fraction where some mixing of lipid rafts and other cellular components occurs. The phenomena that membranes from different cell lines have different average densi-

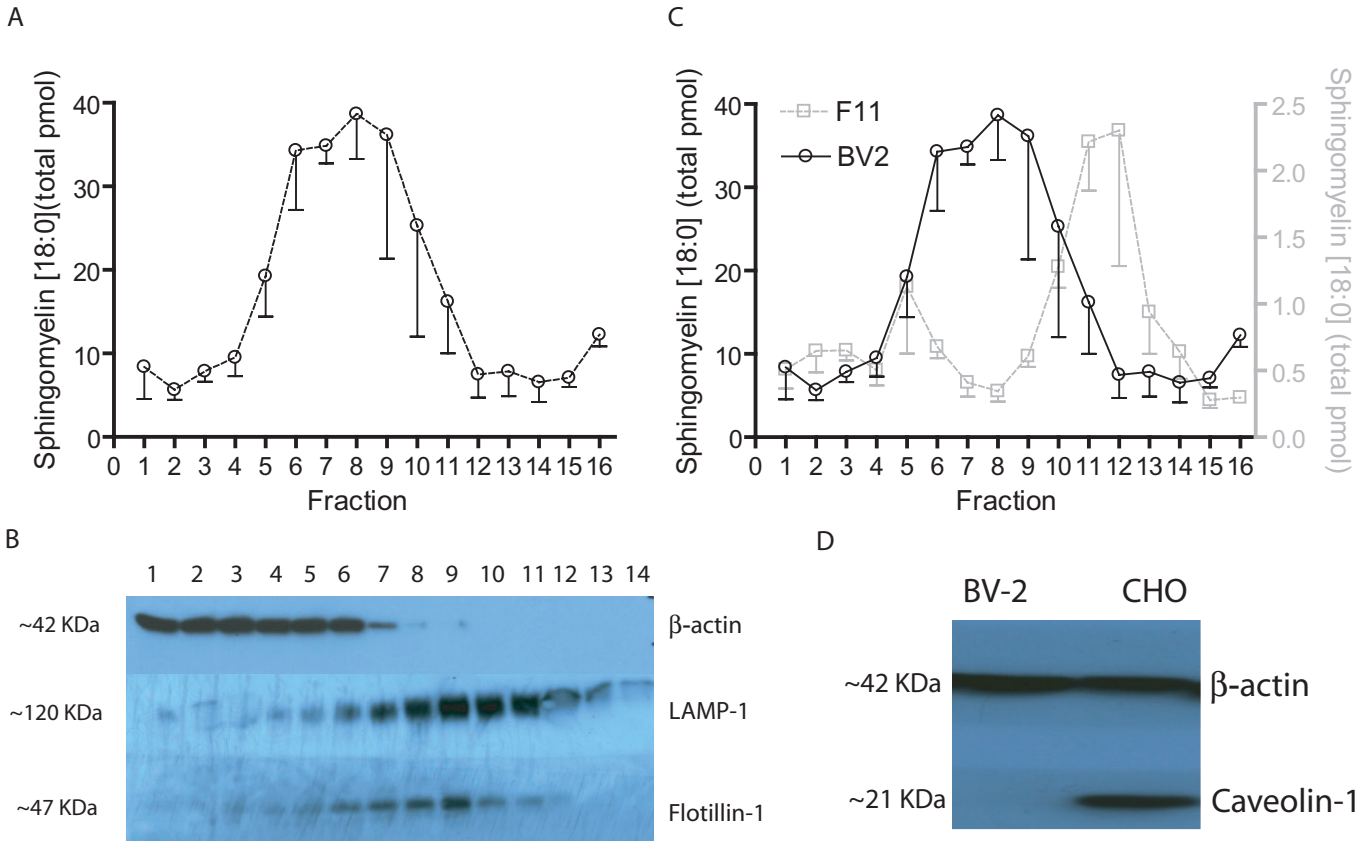

Figure 1

Distribution of membrane raft markers across BV-2 fractions. (A) [18:0]-sphingomyelin is highest in fraction 8 (significantly different from fractions 1–5, and 11–16, $P < 0.05$, $n = 3$; one-way ANOVA, Fisher's LSD *post hoc*). Data are presented as the total quantity in picomoles (pmol) recovered from each fraction. Error bars represent standard error of the mean. (B) Western blot showing the distribution of flotillin-1, LAMP-1, and β-actin. The membrane raft marker flotillin-1 is concentrated in fractions 6–10. β-actin is localized mostly to fractions 1–7, with small amounts in the lighter fractions 8–9. LAMP-1, a lysosomal marker is spread through the lipid rafts and lighter fractions 6–13. (C) Comparison of [18:0]-sphingomyelin distribution between BV-2 (left *y*-axis) and F-11 (right *y*-axis) cells. Data for F-11 cells (from Rimmerman *et al.* 2008) was re-plotted in picomoles. (D) Western blot showing that BV-2 cells are devoid of the protein caveolin-1, CHO cells serve as a positive control.

ties, resulting in lipid rafts and other membranes to be recovered at slightly shifted positions on the density gradient, was previously reported (Macdonald and Pike, 2005). Figure 1C shows a comparison of the distribution of the lipid raft marker [18:0]-sphingomyelin in both cell lines. β-actin, a cytoskeletal protein associated with both raft and non-raft fractions was observed in high concentrations in non-lipid raft fractions, and found in low levels in lipid raft fractions (Figure 1B). The lysosomal marker LAMP-1 was found in the lipid raft fractions as previously reported (Figure 1B; Zhai *et al.*, 2009). The membrane raft protein caveolin-1, which was shown to be associated with the caveolae lipid raft subtype and necessary for their formation (Drab *et al.*, 2001) was absent from BV-2 cells (Figure 1D). Caveolin-1 was present in CHO cells (Figure 1D), F11 cells (Rimmerman *et al.*, 2008) and human endothelial cells (data not shown). qPCR analysis demonstrated that BV-2 cells were negative for caveolin-1 mRNA (no reaction product was obtained after 40 PCR cycles; mouse primary astrocytes were used as positive control). BV-2 cells were found to express caveolin-2 mRNA (reaction product appeared after 22 cycles).

Compartmentalization of endocannabinoids in BV-2 cells

2-AG levels in control cells were highest in the lipid raft fractions (6–9; Figure 2A) as previously shown by us for the F-11 cells, albeit with a general leftward shift of lipid raft fractions on the density gradient when compared with F-11 cells (Figure 2B; Rimmerman *et al.*, 2008). The other endocannabinoid, AEA, was present in both lipid raft and non-lipid raft fractions (Figure 2C). Owing to the low levels of AEA, it was not possible to detect it in all of the fractions. Western blot analysis revealed localization of CB_2 receptors and of the vanilloid receptor TRPV2 to non-raft fractions (Figure 2D). High levels of CB_1 receptors were localized to the high-density non-lipid raft fractions, while smaller amounts were found through the lipid raft fractions (Figure 2D). The localization of CB_1 receptors (and other proteins) between

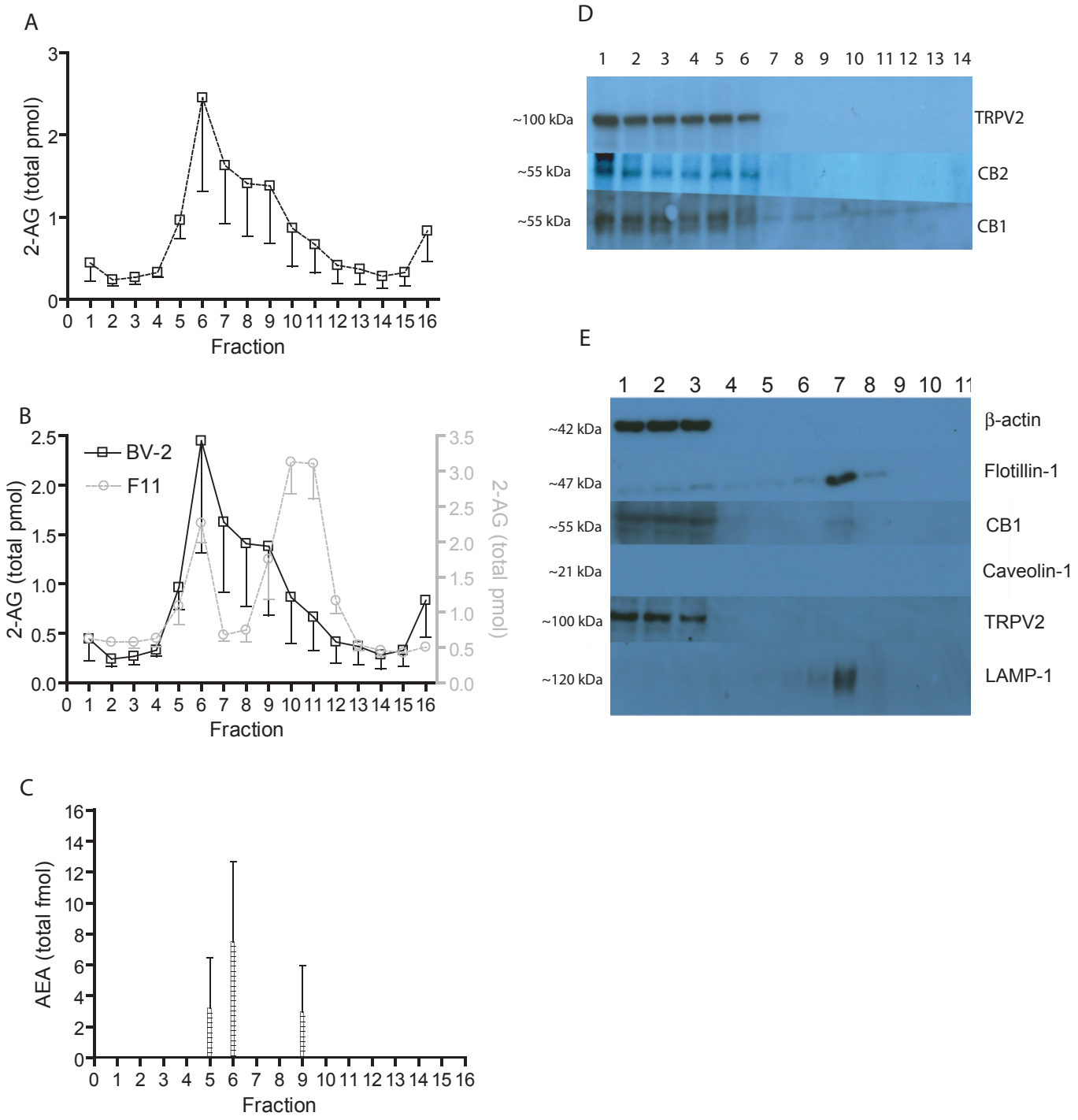

Figure 2

Distribution of endocannabinoids and CB receptors across BV-2 fractions. (A) 2-AG (in pmol) is highest in interface fraction 6, and significantly different from fractions 1–5 and 10–16 ($P < 0.05$, $n = 3$, one-way ANOVA, Fisher's LSD *post hoc*). (B) Comparison of 2-AG distribution between BV-2 (left *y*-axis) and F-11 (right *y*-axis) cells. Data for F-11 cells was re-plotted from Rimmerman *et al.* (2008). (C) AEA is found in non-lipid raft fraction 5, 6 and lipid raft fraction 9. (D) CB_2 receptors and the vanilloid receptor TRPV2 are localized to non-lipid raft fractions 1–5 and interface fraction 6. CB_1 receptors are present mostly in non-lipid raft fractions 1–5 and 6. Small amounts are present in lipid raft fractions. (E) Western blot analysis of fractions obtained using a second fractionation method confirmed the compartmentalization of β-actin, TRPV2 and most of CB_1 receptors in the non-lipid raft fractions. Flotillin-1, LAMP-1 and part of the CB_1 receptors are present in lipid raft fractions. Caveolin-1 is not found in any of the fractions. These results are consistent with the OptiPrep fractionation method.

non-lipid rafts and lipid rafts was verified by a second fractionation method (Song *et al.*, 1996; Ostrom *et al.*, 2001) which showed similar results (Figure 2E), i.e., the presence of flotillin-1, LAMP-1, small amounts of CB_1 receptor and lack of caveolin-1 in lipid rafts isolated from BV-2 cells.

Three NAEs: OEA, PEA and SEA showed a distribution similar to that of 2-AG. Specifically, OEA and PEA levels were highest in the interface fraction 6 and in the lipid raft fractions 7–9 (their levels were lower in fractions 1–5 and 10–16 (Figures 3A, B, $P < 0.05$, $n = 3$, one-way ANOVA, Fisher's LSD *post hoc*). SEA was highest in interface fraction 6 which was significantly different from fractions 1–4 and 10–16 (Figures 3C, $P < 0.05$, $n = 3$, one-way ANOVA, Fisher's LSD *post hoc*).

Compartmentalization of endocannabinoids following treatment with CBD

Treatment with CBD (10 μM) for 3 h did not change the distribution pattern of the lipid raft marker [18:0]-sphingomyelin, or protein marker flotillin-1 (Figure 4A, C). CBD was localized to interface fraction 6 and to a lesser degree to lipid raft fraction 7 (Figure 4B). The distribution of β-actin, LAMP-1, CB_1, CB_2 and, TRPV2 was not affected by CBD (Figure 4C). Similarly, levels and distribution of 2-AG and AEA were equivalent to vehicle-treated cells (Figure 5A, B). However, following CBD treatment, the level of OEA in lipid rafts was not increased (Figure 6A), whereas the saturated NAEs, PEA and SEA were significantly increased in lipid raft fractions, demonstrating a shift towards the lighter fractions (Figure 6B, C).

In order to investigate the kinetics of the CBD-induced changes in 2-AG and NAEs levels, cells were incubated with vehicle or CBD and analysed for lipid content (including growth medium) at different time points (10, 30, 60, and 210 min). 2-AG levels in whole cells + growth medium did not change following CBD treatment (Figure 7A). Conversely, AEA levels were significantly increased in whole cells with growth medium at 60 and 210 min compared with vehicle-treated cells (Figure 7B). OEA levels were also significantly increased in whole cells with growth medium at 60 and 210 min compared with vehicle-treated cells (Figure 7C), whereas PEA and SEA levels were not markedly increased (Figure 7D, E).

Discussion

Microglia are resident macrophages that serve as early host defence against pathogens in the CNS. Chronic activation of microglial cells seems to be a major factor in the development of neuroinflammation and contributes to neuronal damage and pathology associated with neurodegeneration (Farooqui *et al.*, 2007). The murine BV-2 cell line is a useful model of microglial cells (Blasi *et al.*, 1990; Bocchini *et al.*, 1992), and we recently showed that CBD inhibits the anti-inflammatory response and alters gene expression of stress genes in these cells (Kozela *et al.*, 2010; Juknat *et al.*, 2012). Additionally, BV-2 cells express a functional cannabinoid system including related receptors: CB_1, CB_2, GPR55, GPR18, the metabolic enzymes: ABHD6 and FAAH, the endocannabinoids 2-AG and

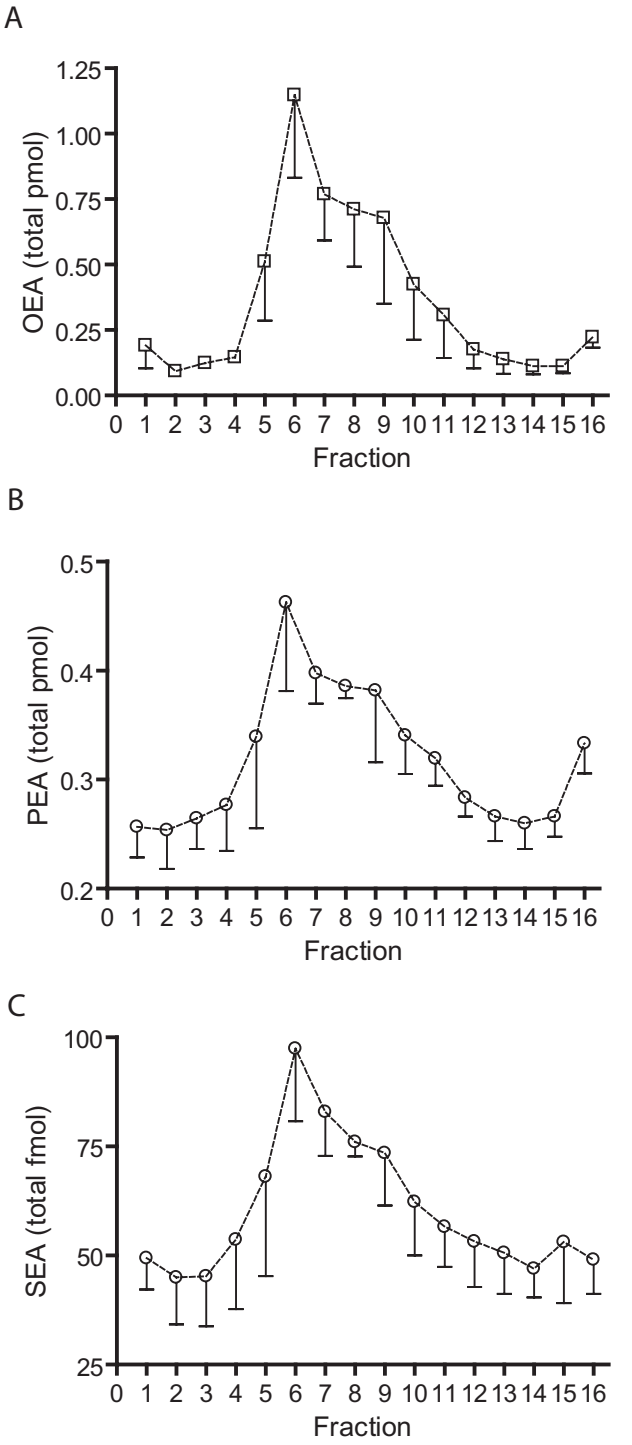

Figure 3

Distribution of the NAEs, OEA, PEA and SEA, across BV-2 fractions. (A) OEA levels are highest in interface fraction 6 which is significantly different from fractions 1–5 and 10–16 ($P < 0.05$, $n = 3$, one-way ANOVA, Fisher's LSD *post hoc*). (B) PEA levels are highest in interface fraction 6 which is significantly different from fractions 1–5 and 10–16 ($P < 0.05$, $n = 3$, one-way ANOVA, Fisher's LSD *post hoc*).(C) SEA is highest in interface fraction 6 which is significantly different from fractions 1–4 and 10–16 ($P < 0.05$, $n = 3$, one-way ANOVA, Fisher's LSD *post hoc*).

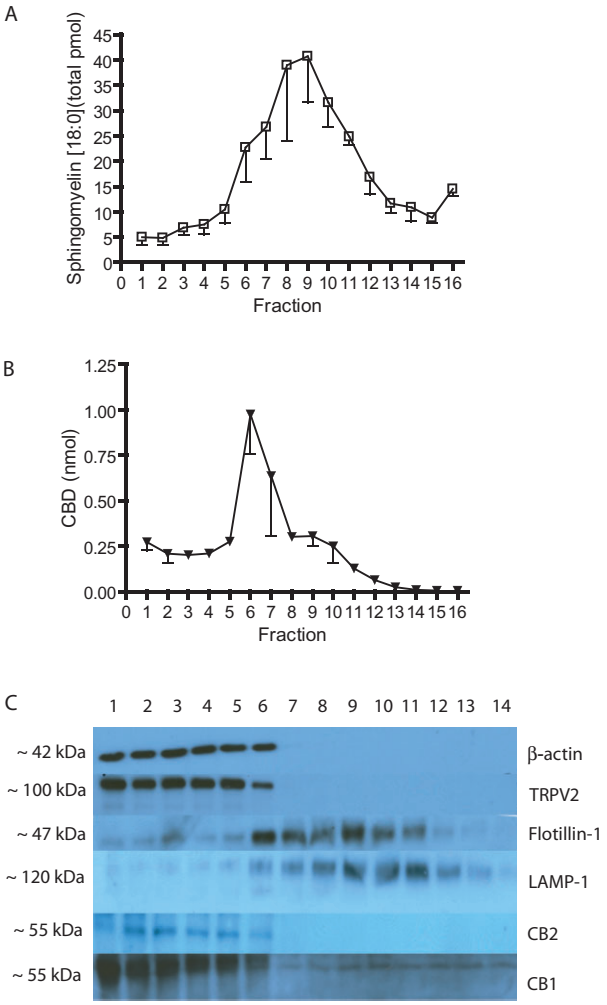

Figure 4

Distribution of membrane raft markers and CBD across BV-2 fractions following CBD treatment. (A) [18:0]-sphingomyelin is highest in fraction 9 (significantly different from fractions 1–6, and 12–16, $P < 0.05$, $n = 3$; one-way ANOVA, Fisher's LSD *post hoc*). (B) CBD is highest in fractions 6 and 7 (CBD levels found in fraction 6 are significantly different from fractions 1–5 and 8–16; $P < 0.02$; $n = 3$, one-way ANOVA, Fisher's LSD *post hoc*). (C) Lipid raft marker flotillin-1 is concentrated in fractions 6–11. β-actin is localized mostly to fractions 1–6. LAMP-1 is spread through lipid rafts and the lighter fractions 6–14. CB_2 receptors and the vanilloid receptor TRPV2 are localized to non-membrane raft fractions 1–5, and interface fraction 6. CB_1 receptors are compartmentalized mainly to non-lipid raft fractions with small amounts appearing in lipid raft fractions.

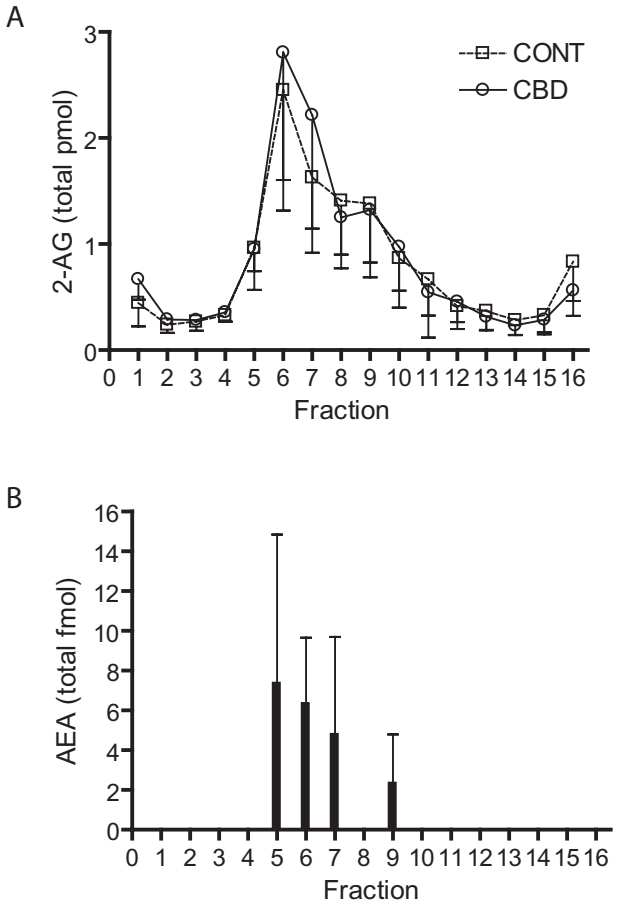

Figure 5

Distribution of the endocannabinoids AEA and 2-AG across BV-2 fractions following CBD treatment. (A) 2-AG levels and distribution are not affected by CBD treatment. (B) Following CBD treatment, AEA was found in the heavier fraction 5, interface fraction 6, and lipid raft fractions (7 and 9).

AEA, and other NAEs (Pietr *et al.*, 2009; Stella, 2009; Marrs *et al.*, 2010; McHugh *et al.*, 2010).

Compartmentalization of 2-AG and NAEs in membrane domains is not well characterized, and lipid raft/caveolae are emerging as important domains involved in their signal transduction (McFarland *et al.*, 2004; 2008; Bari *et al.*, 2005a,b; 2006; 2008; McFarland and Barker, 2005; Sarnataro *et al.*, 2005, 2006; Oddi *et al.*, 2007; Placzek *et al.*, 2008; Rimmerman *et al.*, 2008; Yates and Barker, 2009; Maccarrone *et al.*, 2010). We previously investigated the compartmentalization of endocannabinoid signalling in F-11 cells which served as a model of peripheral neurons. Here, we report that the lipid rafts of F-11 cells and of BV-2 cells show different densities, and appear in slightly different locations on the gradient (using identical density gradient methodology). Lipid rafts in the F-11 cells are well separated from non-lipid raft fractions (forming two separate peaks). In contrast, BV-2 lipid raft fractions exhibit a higher density as evident by the localization of lipid raft markers, flotillin-1 and sphingomyelin. The fact that membranes from different cells exhibit altered average densities has been previously reported (Macdonald and Pike, 2005). Differences in protein expression and lipid composition may explain these differences. Indeed, we find that BV-2 cells, in contrast to F-11 cells, are devoid of caveolin-1. Caveolin-1, which is necessary for the formation of caveolae, was reported to modulate cholesterol transport (Murata *et al.*, 1995; Ikonen and Parton, 2000). Pike *et al.* (2002) reported that human epidermal carcinoma cells devoid of caveolin-1 had significantly reduced cholesterol

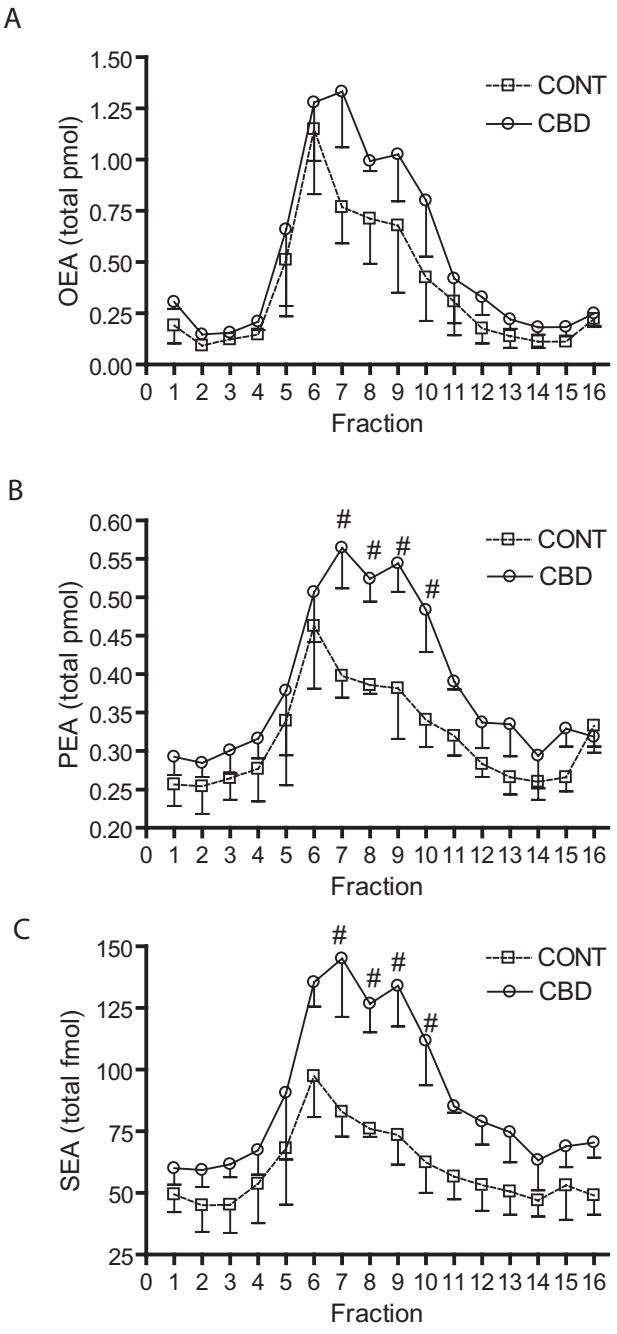

Figure 6

Distribution of the NAEs, PEA, SEA, and OEA across BV-2 fractions following CBD treatment. (A) OEA levels are highest in fraction 7 in the CBD-treated cells and are significantly different from fractions 1–5 and 10–16 ($P < 0.05$; $n = 3$, one-way ANOVA, Fisher's LSD *post hoc*. The levels of OEA are not significantly increased in CBD-treated cells compared with vehicle-treated cells. (B) In CBD-treated cells, PEA peaked in fraction 7 and was increased in fractions 6–10 (fraction 7 is significantly different from fractions 1–5 and 11–16; $P < 0.02$; $n = 3$, one-way ANOVA, Fisher's LSD *post hoc*). Lipid raft fractions 7–10 in CBD-treated cells have significantly increased levels of PEA when compared with vehicle-treated cells (#, fraction 7, $P < 0.03$; fraction 8, $P < 0.06$; fraction 9, $P < 0.03$; fraction 10, $P < 0.05$; $n = 3$, one-way ANOVA, Fisher's LSD *post hoc*). (C) SEA levels are highest in fraction 7 in the CBD-treated cells and are significantly different from fractions 1–5 and 11–16, $P < 0.01$; $n = 3$, one-way ANOVA, Fisher's LSD *post hoc*). Lipid raft fractions (7–10) in the CBD-treated cells have significantly increased levels of SEA (fraction 7, $P < 0.005$; fraction 8, $P < 0.02$; fraction 9, $P < 0.05$; fraction 10, $P < 0.02$; $n = 3$, one-way ANOVA, Fisher's LSD *post hoc*).

levels compared with human epidermal carcinoma cells which had been transfected with mouse caveolin-1. Such differences in protein lipid content (e.g. caveolin-1 and cholesterol) may contribute to the density differences observed between F-11 and BV-2 lipid rafts.

Compartmentalization of 2-AG in BV-2 lipid rafts

In F-11 cells, endogenous 2-AG was concentrated in lipid raft fractions, where its levels were significantly higher than in any other fraction. The non-lipid raft fractions contained much lower levels of 2-AG. A similar phenomenon was observed in the BV-2 cells. Incubation of BV-2 cells with CBD did not change the distribution or levels of 2-AG between fractions. Whole cells with growth medium levels were also not affected by the CBD treatment, and the synthetic enzyme DGLα was below our detection limit using Western blot analysis. To conclude, 2-AG has a high affinity for lipid rafts in two cell lines, and CBD did not affect 2-AG metabolism or synthesis in BV-2 cells.

Compartmentalization of NAEs in BV-2 lipid rafts

We previously investigated the compartmentalization of AEA in F-11 fractions and found that AEA was present in significant levels in both lipid raft and non- lipid raft fractions. Using deuterium-labelled AEA, we determined that deuterium-labeled free arachidonic acid, a direct metabolic product of AEA hydrolysis, was found in non-lipid raft fractions. We postulated that AEA was endocytosed and trafficked to be hydrolysed in non-lipid raft FAAH-containing membranes. This is consistent with the proposed theory of lipid raft/caveolae-mediated AEA endocytosis (McFarland and Barker, 2005). AEA levels in several of the BV-2 membrane fractions were below our detection limit. Wherever AEA was detectable, significant levels were measured in both lipid rafts and non-lipid raft fractions (similar to AEA distribution in F-11 cells). Remarkably, AEA levels in whole cells with growth medium were significantly increased following CBD treatment in a time-dependent manner. Because the levels of AEA in membrane fractions cannot account for these changes, we hypothesize that excess AEA production following CBD treatment is released into the growth medium.

The CB_1 receptor was previously compartmentalized in lipid raft/caveolae membranes in several cellular systems (Keren and Sarne, 2003; Bari *et al.*, 2005b; 2006; 2008; Sarnataro *et al.*, 2005; 2006). In BV-2 cell fractions, we observed compartmentalization of CB_1 receptors mostly to non-lipid raft membranes. Using two different fractionation methods we show that only small amounts of CB_1 receptors are localized to lipid rafts. It is yet to be determined whether association of CB_1 receptors with BV-2 lipid rafts is affected by the

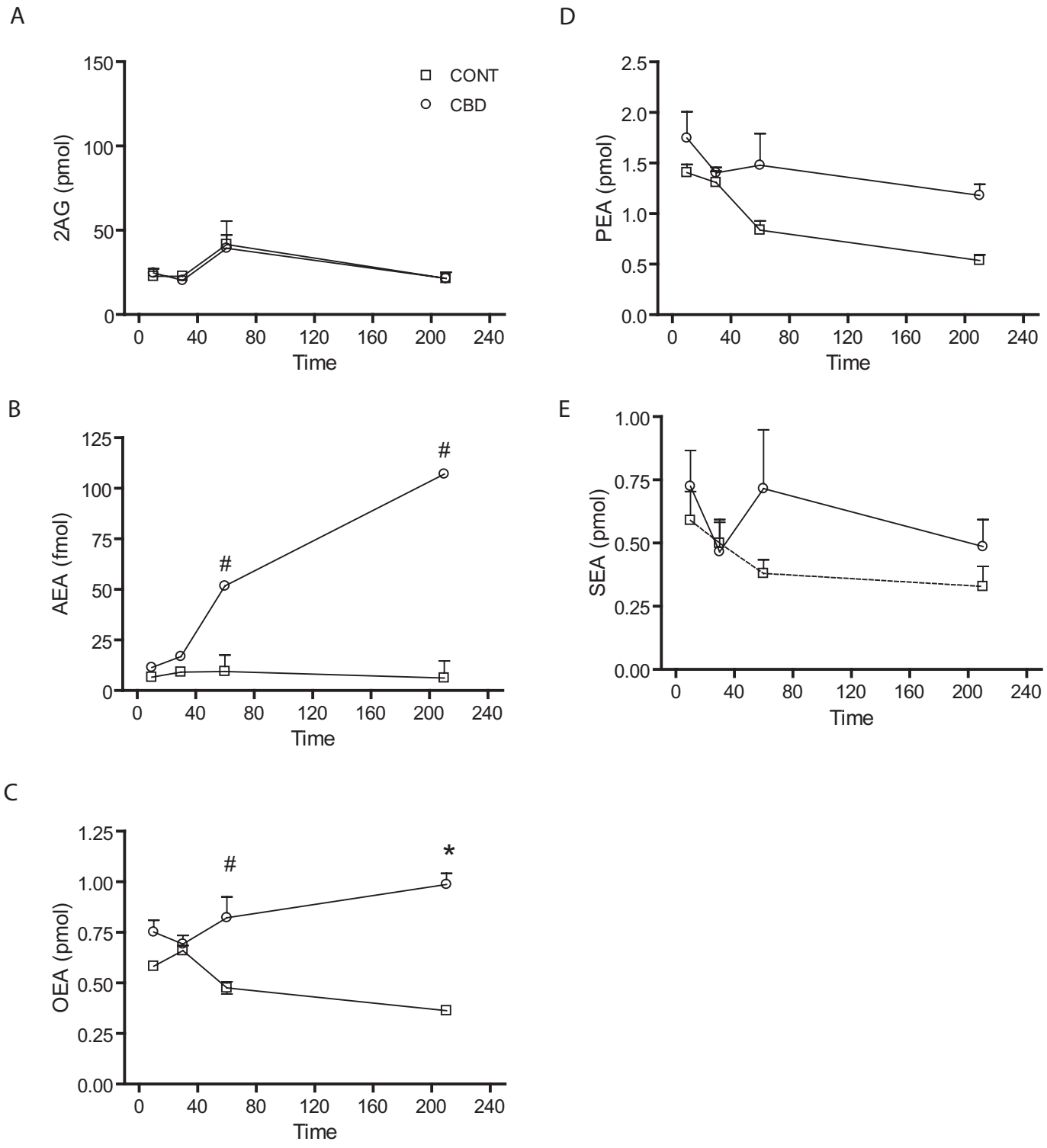

Figure 7

2-AG and NAE levels in whole cells + media, following CBD treatment. (A) 2-AG levels in whole cells + growth medium are not significantly different between CBD-treated and vehicle-treated cells. (B) AEA levels are increased in whole cells + growth medium from CBD-treated cells at 60 min and 210 min, #, $P < 0.001$; $n = 3$, at CBD 210 min, $n = 2$, Bonferroni *post hoc*. (C) OEA levels are increased in whole cells + growth medium from CBD-treated cells compared with control at 60 min #, $P < 0.02$; at 210 min, *$P < 0.001$; $n = 3$ (at CBD 210 min, $n = 2$), one-way ANOVA, Bonferroni *post hoc*. (D) PEA levels in whole cells + growth medium are not significantly different between CBD-treated and vehicle-treated cells. (E) SEA levels in whole cells + growth medium are not significantly different between CBD-treated and vehicle-treated cells.

lack of caveolin-1, which may well affect cholesterol balance in the cells. This association may explain apparent differences in lipid raft localization of CB_1 receptors between cell types. Consistent with previous reports, CB_2 receptors did not compartmentalize in lipid rafts (Bari *et al.*, 2006; Rimmerman *et al.*, 2008).

Levels of the monounsaturated *N*-acyl ethanolamine derivative OEA showed a similar trend to AEA. OEA levels in the membrane fractions showed a slight, non-significant increase following CBD treatment. However, OEA levels in whole cells with growth medium were significantly increased following CBD incubation in a time-dependent manner. The accumulation of AEA and OEA in whole cells with growth medium following CBD treatment, suggests that CBD is inhibiting their uptake and/or hydrolysis. Although AEA uptake has been extensively investigated, not much is known about the uptake of OEA (Di Marzo *et al.*, 1994; Beltramo *et al.*, 1997; Bisogno *et al.*, 1997; 2001b; Jacobsson and Fowler, 2001; Fowler and Jacobsson, 2002; McFarland and Barker, 2005; Hermann *et al.*, 2006; Thors *et al.*, 2007; Placzek *et al.*, 2008; Kaczocha *et al.*, 2006; 2009; Oddi *et al.*, 2008; 2009; Maccarrone *et al.*, 2010). In contrast, the mechanisms of NAE hydrolysis have been determined (Cravatt *et al.*, 1996). In this context, CBD was previously shown to inhibit AEA uptake and hydrolysis in several systems. For example, CBD inhibited AEA hydrolysis in mouse brain microsomes (Watanabe *et al.*, 1996). In addition, CBD inhibited AEA uptake by RBL-2H3 with K_i ~ 11 μM (Rakhshan *et al.*, 2000). Furthermore, Bisogno *et al.* (2001a) reported that CBD inhibited [^{14}C]-AEA uptake in RBL-2H3 cells (IC_{50} of 22 μM), and [^{14}C]-AEA hydrolysis in N18TG2 cell membranes (IC_{50} of 27.5 μM). Different results were reported by Massi *et al.* (2008) where CBD stimulated the activity of FAAH, and decreased AEA content in tumors from CBD-treated nude mice, and in U87 human glioma cells. Our results in BV-2 cells support the reported inhibition by CBD of AEA uptake and/or hydrolysis, and extend it to OEA. Additionally, we showed that following CBD treatment, the levels of the saturated NAEs, PEA and SEA significantly increased in lipid raft fractions. This is also consistent with an inhibitory effect of CBD on NAE metabolism and the compartmentalization of this accumulation to lipid rafts. We also found that CBD treatment did not affect 2-AG levels, consistent with the findings of Marrs *et al.* (2010) showing that 2-AG hydrolysis in intact cells proceeds through the enzyme ABHD6 rather than FAAH. Aside from the effects of CBD on FAAH activity, there may be other mechanisms leading to the increased accumulation of NAEs. For example, we have found that CBD increased, by 90%, the mRNA level of the enzyme protein tyrosine phosphatase, non receptor 22 (PTPN22) (Rimmerman, unpublished experiments), which was shown to be involved in AEA synthesis from phospho-AEA in a macrophage cell line (Liu *et al.*, 2006).

CBD was previously shown to exert immunosuppressive effects on immune cells *in vitro* and *in vivo* (Ignatowska-Jankowska *et al.*, 2009; Kozela *et al.*, 2010; 2011; Ruiz-Valdepenas *et al.*, 2011). It is not clear whether the immunosuppressive effects of CBD are mediated via the CBD-induced increases in NAEs, and the NAEs differential compartmentalization. At least for AEA, immunosuppressive effects through the CB_2 receptor have been described (Centioni *et al.*, 2010; Correa *et al.*, 2011). Additional research will be needed to determine the contribution of NAEs compartmentalization to immune function.

In conclusion, CBD treatment generally increased NAEs accumulation in BV-2 cells. The increase in NAE accumulation may be explained by inhibition of FAAH and/or NAE uptake, induced by CBD. We report that following CBD treatment, NAEs undergo different compartmentalization, depending on the saturation of the fatty acid. The saturated NAEs (PEA and SEA) markedly increased in lipid raft fractions, while the unsaturated NAEs (AEA and OEA) markedly increased in whole cells with growth medium, probably via release to the medium. Our results support the idea that although NAE levels are controlled by similar enzymatic mechanisms, they compartmentalize and signal via divergent pathways. In addition, we hypothesize that the anti-inflammatory effects of CBD may be mediated by the increased accumulation of anti-inflammatory NAEs in microglial cells.

Acknowledgements

This work was supported by the Dr Miriam and Sheldon G. Adelson Medical Research Foundation. A.J and N.R. were supported by the Israeli Center for Absorption in Science.

Conflicts of interest

The authors state no conflict of interest.

References

Alexander SPH, Mathie A, Peters JA (2011). Guide to Receptors and Channels (GRAC), 5th Edition. Br J Pharmacol 164 (Suppl. 1): S1–S324.

Bari M, Battista N, Fezza F, Finazzi-Agro A, Maccarrone M (2005a). Lipid rafts control signaling of type-1 cannabinoid receptors in neuronal cells. Implications for anandamide-induced apoptosis. J Biol Chem 280: 12212–12220.

Bari M, Paradisi A, Pasquariello N, Maccarrone M (2005b). Cholesterol-dependent modulation of type 1 cannabinoid receptors in nerve cells. J Neurosci Res 81: 275–283.

Bari M, Spagnuolo P, Fezza F, Oddi S, Pasquariello N, Finazzi-Agro A *et al.* (2006). Effect of lipid rafts on Cb2 receptor signaling and 2-arachidonoyl-glycerol metabolism in human immune cells. J Immunol 177: 4971–4980.

Bari M, Oddi S, De Simone C, Spagnolo P, Gasperi V, Battista N *et al.* (2008). Type-1 cannabinoid receptors colocalize with caveolin-1 in neuronal cells. Neuropharmacology 54: 45–50.

Barnett-Norris J, Lynch D, Reggio PH (2005). Lipids, lipid rafts and caveolae: their importance for GPCR signaling and their centrality to the endocannabinoid system. Life Sci 77: 1625–1639.

Beltramo M, Stella N, Calignano A, Lin SY, Makriyannis A, Piomelli D (1997). Functional role of high-affinity anandamide transport, as revealed by selective inhibition. Science 277: 1094–1097.

Bisogno T, Maurelli S, Melck D, De Petrocellis L, Di Marzo V (1997). Biosynthesis, uptake, and degradation of anandamide and palmitoylethanolamide in leukocytes. J Biol Chem 272: 3315–3323.

Bisogno T, Hanus L, De Petrocellis L, Tchilibon S, Ponde DE, Brandi I *et al*. (2001a). Molecular targets for cannabidiol and its synthetic analogues: effect on vanilloid VR1 receptors and on the cellular uptake and enzymatic hydrolysis of anandamide. Br J Pharmacol 134: 845–852.

Bisogno T, MacCarrone M, De Petrocellis L, Jarrahian A, Finazzi-Agro A, Hillard C *et al*. (2001b). The uptake by cells of 2-arachidonoylglycerol, an endogenous agonist of cannabinoid receptors. Eur J Biochem 268: 1982–1989.

Blasi E, Barluzzi R, Bocchini V, Mazzolla R, Bistoni F (1990). Immortalization of murine microglial cells by a v-raf/v-myc carrying retrovirus. J Neuroimmunol 27: 229–237.

Bocchini V, Mazzolla R, Barluzzi R, Blasi E, Sick P, Kettenmann H (1992). An immortalized cell line expresses properties of activated microglial cells. J Neurosci Res 31: 616–621.

Bradshaw HB, Rimmerman N, Krey JF, Walker JM (2006). Sex and hormonal cycle differences in rat brain levels of pain-related cannabimimetic lipid mediators. Am J Physiol Regul Integr Comp Physiol 291: R349–R358.

Butovsky E, Juknat A, Elbaz J, Shabat-Simon M, Eilam R, Zangen A *et al*. (2006). Chronic exposure to Delta9-tetrahydrocannabinol downregulates oxytocin and oxytocin-associated neurophysin in specific brain areas. Mol Cell Neurosci 31: 795–804.

Cencioni MT, Chiurchiu V, Catanzaro G, Borsellino G, Bernardi G, Battistini L *et al*. (2010). Anandamide suppresses proliferation and cytokine release from primary human T-lymphocytes mainly via CB2 receptors. PLoS One 5: e8688.

Chini B, Parenti M (2004). G-protein coupled receptors in lipid rafts and caveolae: how, when and why do they go there? J Mol Endocrinol 32: 325–338.

Correa F, Hernangomez-Herrero M, Mestre L, Loria F, Docagne F, Guaza C (2011). The endocannabinoid anandamide downregulates IL-23 and IL-12 subunits in a viral model of multiple sclerosis: evidence for a cross-talk between IL-12p70/IL-23 axis and IL-10 in microglial cells. Brain Behav Immun 25: 736–749.

Cravatt BF, Giang DK, Mayfield SP, Boger DL, Lerner RA, Gilula NB (1996). Molecular characterization of an enzyme that degrades neuromodulatory fatty-acid amides. Nature 384: 83–87.

Czarny M, Lavie Y, Fiucci G, Liscovitch M (1999). Localization of phospholipase D in detergent-insoluble, caveolin-rich membrane domains. Modulation by caveolin-1 expression and caveolin-182-101. J Biol Chem 274: 2717–2724.

Di Marzo V, Fontana A, Cadas H, Schinelli S, Cimino G, Schwartz JC *et al*. (1994). Formation and inactivation of endogenous cannabinoid anandamide in central neurons. Nature 372: 686–691.

Drab M, Verkade P, Elger M, Kasper M, Lohn M, Lauterbach B *et al*. (2001). Loss of caveolae, vascular dysfunction, and pulmonary defects in caveolin-1 gene-disrupted mice. Science 293: 2449–2452.

Farooqui AA, Horrocks LA, Farooqui T (2007). Modulation of inflammation in brain: a matter of fat. J Neurochem 101: 577–599.

Fay JF, Dunham TD, Farrens DL (2005). Cysteine residues in the human cannabinoid receptor: only C257 and C264 are required for a functional receptor, and steric bulk at C386 impairs antagonist SR141716A binding. Biochemistry 44: 8757–8769.

Fielding CJ, Fielding PE (1997). Intracellular cholesterol transport. J Lipid Res 38: 1503–1521.

Fielding PE, Fielding CJ (1995). Plasma membrane caveolae mediate the efflux of cellular free cholesterol. Biochemistry 34: 14288–14292.

Fowler CJ, Jacobsson SO (2002). Cellular transport of anandamide, 2-arachidonoylglycerol and palmitoylethanolamide–targets for drug development? Prostaglandins Leukot Essent Fatty Acids 66: 193–200.

Franklin A, Parmentier-Batteur S, Walter L, Greenberg DA, Stella N (2003). Palmitoylethanolamide increases after focal cerebral ischemia and potentiates microglial cell motility. J Neurosci 23: 7767–7775.

Fu J, Oveisi F, Gaetani S, Lin E, Piomelli D (2005). Oleoylethanolamide, an endogenous PPAR-alpha agonist, lowers body weight and hyperlipidemia in obese rats. Neuropharmacology 48: 1147–1153.

Gaus K, Gratton E, Kable EP, Jones AS, Gelissen I, Kritharides L *et al*. (2003). Visualizing lipid structure and raft domains in living cells with two-photon microscopy. Proc Natl Acad Sci U S A 100: 15554–15559.

Godlewski G, Offertaler L, Wagner JA, Kunos G (2009). Receptors for acylethanolamides-GPR55 and GPR119. Prostaglandins Other Lipid Mediat 89: 105–111.

Hansen HS (2010). Palmitoylethanolamide and other anandamide congeners. Proposed role in the diseased brain. Exp Neurol 224: 48–55.

Hermann A, Kaczocha M, Deutsch DG (2006). 2-Arachidonoylglycerol (2-AG) membrane transport: history and outlook. Aaps J 8: E409–E412.

Ignatowska-Jankowska B, Jankowski M, Glac W, Swiergel AH (2009). Cannabidiol-induced lymphopenia does not involve NKT and NK cells. J Physiol Pharmacol 60 (Suppl. 3): 99–103.

Ikonen E, Parton RG (2000). Caveolins and cellular cholesterol balance. Traffic 1: 212–217.

Jacobsson SO, Fowler CJ (2001). Characterization of palmitoylethanolamide transport in mouse Neuro-2a neuroblastoma and rat RBL-2H3 basophilic leukaemia cells: comparison with anandamide. Br J Pharmacol 132: 1743–1754.

Juknat A, Pietr M, Kozela E, Rimmerman N, Levy L, Coppola G *et al*. (2012). Differential transcriptional profiles mediated by exposure to the cannabinoids cannabidiol and Δ9-tetrahydrocannabinol in BV-2 microglial cells. Br J Pharmacol 165: 2512–2528.

Kaczocha M, Hermann A, Glaser ST, Bojesen IN, Deutsch DG (2006). Anandamide uptake is consistent with rate-limited diffusion and is regulated by the degree of its hydrolysis by fatty acid amide hydrolase. J Biol Chem 281: 9066–9075.

Kaczocha M, Glaser ST, Deutsch DG (2009). Identification of intracellular carriers for the endocannabinoid anandamide. Proc Natl Acad Sci U S A 106: 6375–6380.

Keren O, Sarne Y (2003). Multiple mechanisms of CB1 cannabinoid receptors regulation. Brain Res 980: 197–205.

Kozela E, Pietr M, Juknat A, Rimmerman N, Levy R, Vogel Z (2010). Cannabinoids Delta(9)-tetrahydrocannabinol and cannabidiol differentially inhibit the lipopolysaccharide-activated NF-kappaB and interferon-beta/STAT proinflammatory pathways in BV-2 microglial cells. J Biol Chem 285: 1616–1626.

Kozela E, Lev N, Kaushansky N, Eilam R, Rimmerman N, Levy R *et al.* (2011). Cannabidiol inhibits pathogenic T-cells, decreases spinal microglial activation and ameliorates multiple sclerosis-like disease in C57BL/6 mice. Br J Pharmacol 163: 1507–1519.

Lajoie P, Nabi IR (2010). Lipid rafts, caveolae, and their endocytosis. Int Rev Cell Mol Biol 282: 135–163.

Liu J, Wang L, Harvey-White J, Osei-Hyiaman D, Razdan R, Gong Q *et al.* (2006). A biosynthetic pathway for anandamide. Proc Natl Acad Sci U S A 103: 13345–13350.

Lo Verme J, Fu J, Astarita G, La Rana G, Russo R, Calignano A *et al.* (2005a). The nuclear receptor peroxisome proliferator-activated receptor-alpha mediates the anti-inflammatory actions of palmitoylethanolamide. Mol Pharmacol 67: 15–19.

Lo Verme J, Gaetani S, Fu J, Oveisi F, Burton K, Piomelli D (2005b). Regulation of food intake by oleoylethanolamide. Cell Mol Life Sci 62: 708–716.

Luo DX, Cao DL, Xiong Y, Peng XH, Liao DF (2010). A novel model of cholesterol efflux from lipid-loaded cells. Acta Pharmacol Sin 31: 1243–1257.

Maccarrone M, Pauselli R, Di Rienzo M, Finazzi-Agro A (2002). Binding, degradation and apoptotic activity of stearoylethanolamide in rat C6 glioma cells. Biochem J 366: 137–144.

Maccarrone M, De Chiara V, Gasperi V, Viscomi MT, Rossi S, Oddi S *et al.* (2009). Lipid rafts regulate 2-arachidonoylglycerol metabolism and physiological activity in the striatum. J Neurochem 109: 371–381.

Maccarrone M, Dainese E, Oddi S (2010). Intracellular trafficking of anandamide: new concepts for signaling. Trends Biochem Sci 35: 601–608.

Macdonald JL, Pike LJ (2005). A simplified method for the preparation of detergent-free lipid rafts. J Lipid Res 46: 1061–1067.

Marrs WR, Blankman JL, Horne EA, Thomazeau A, Lin YH, Coy J *et al.* (2010). The serine hydrolase ABHD6 controls the accumulation and efficacy of 2-AG at cannabinoid receptors. Nat Neurosci 13: 951–957.

Massi P, Valenti M, Vaccani A, Gasperi V, Perletti G, Marras E *et al.* (2008). 5-Lipoxygenase and anandamide hydrolase (FAAH) mediate the antitumor activity of cannabidiol, a non-psychoactive cannabinoid. J Neurochem 104: 1091–1100.

McFarland MJ, Barker EL (2005). Lipid rafts: a nexus for endocannabinoid signaling? Life Sci 77: 1640–1650.

McFarland MJ, Porter AC, Rakhshan FR, Rawat DS, Gibbs RA, Barker EL (2004). A role for caveolae/lipid rafts in the uptake and recycling of the endogenous cannabinoid anandamide. J Biol Chem 279: 41991–41997.

McFarland MJ, Bardell TK, Yates ML, Placzek EA, Barker EL (2008). RNA interference-mediated knockdown of dynamin 2 reduces endocannabinoid uptake into neuronal dCAD cells. Mol Pharmacol 74: 101–108.

McHugh D, Hu SS, Rimmerman N, Juknat A, Vogel Z, Walker JM *et al.* (2010). N-arachidonoyl glycine, an abundant endogenous lipid, potently drives directed cellular migration through GPR18, the putative abnormal cannabidiol receptor. BMC Neurosci 11: 44.

Moffett S, Brown DA, Linder ME (2000). Lipid-dependent targeting of G proteins into rafts. J Biol Chem 275: 2191–2198.

Muccioli GG, Stella N (2008). Microglia produce and hydrolyze palmitoylethanolamide. Neuropharmacology 54: 16–22.

Muccioli GG, Xu C, Odah E, Cudaback E, Cisneros JA, Lambert DM *et al.* (2007). Identification of a novel endocannabinoid-hydrolyzing enzyme expressed by microglial cells. J Neurosci 27: 2883–2889.

Mukhopadhyay S, Cowsik SM, Lynn AM, Welsh WJ, Howlett AC (1999). Regulation of Gi by the CB1 cannabinoid receptor C-terminal juxtamembrane region: structural requirements determined by peptide analysis. Biochemistry 38: 3447–3455.

Murata M, Peranen J, Schreiner R, Wieland F, Kurzchalia TV, Simons K (1995). VIP21/caveolin is a cholesterol-binding protein. Proc Natl Acad Sci U S A 92: 10339–10343.

O'Sullivan SE (2007). Cannabinoids go nuclear: evidence for activation of peroxisome proliferator-activated receptors. Br J Pharmacol 152: 576–582.

Oddi S, Spagnuolo P, Bari M, D'Agostino A, Maccarrone M (2007). Differential modulation of type 1 and type 2 cannabinoid receptors along the neuroimmune axis. Int Rev Neurobiol 82: 327–337.

Oddi S, Fezza F, Pasquariello N, De Simone C, Rapino C, Dainese E *et al.* (2008). Evidence for the intracellular accumulation of anandamide in adiposomes. Cell Mol Life Sci 65: 840–850.

Oddi S, Fezza F, Pasquariello N, D'Agostino A, Catanzaro G, De Simone C *et al.* (2009). Molecular identification of albumin and Hsp70 as cytosolic anandamide-binding proteins. Chem Biol 16: 624–632.

Ostrom RS, Gregorian C, Drenan RM, Xiang Y, Regan JW, Insel PA (2001). Receptor number and caveolar co-localization determine receptor coupling efficiency to adenylyl cyclase. J Biol Chem 276: 42063–42069.

Overton HA, Babbs AJ, Doel SM, Fyfe MC, Gardner LS, Griffin G *et al.* (2006). Deorphanization of a G protein-coupled receptor for oleoylethanolamide and its use in the discovery of small-molecule hypophagic agents. Cell Metab 3: 167–175.

Overton HA, Fyfe MC, Reynet C (2008). GPR119, a novel G protein-coupled receptor target for the treatment of type 2 diabetes and obesity. Br J Pharmacol 153 (Suppl. 1): S76–S81.

Pietr M, Kozela E, Levy R, Rimmerman N, Lin YH, Stella N *et al.* (2009). Differential changes in GPR55 during microglial cell activation. FEBS Lett 583: 2071–2076.

Pike LJ (2006). Rafts defined: a report on the Keystone Symposium on Lipid Rafts and Cell Function. J Lipid Res 47: 1597–1598.

Pike LJ, Han X, Chung KN, Gross RW (2002). Lipid rafts are enriched in arachidonic acid and plasmenylethanolamine and their composition is independent of caveolin-1 expression: a quantitative electrospray ionization/mass spectrometric analysis. Biochemistry 41: 2075–2088.

Placzek EA, Okamoto Y, Ueda N, Barker EL (2008). Mechanisms for recycling and biosynthesis of endogenous cannabinoids anandamide and 2-arachidonylglycerol. J Neurochem 107: 987–1000.

Rakhshan F, Day TA, Blakely RD, Barker EL (2000). Carrier-mediated uptake of the endogenous cannabinoid anandamide in RBL-2H3 cells. J Pharmacol Exp Ther 292: 960–967.

Rimmerman N, Hughes HV, Bradshaw HB, Pazos MX, Mackie K, Prieto AL *et al.* (2008). Compartmentalization of endocannabinoids into lipid rafts in a dorsal root ganglion cell line. Br J Pharmacol 153: 380–389.

Rimmerman N, Juknat A, Kozela E, Levy R, Bradshaw HB, Vogel Z (2011). The non-psychoactive plant cannabinoid, cannabidiol affects cholesterol metabolism-related genes in microglial cells. Cell Mol Neurobiol DOI: 10.1007/s10571-011-9692-3 [Epub ahead of print].

Ruiz-Valdepenas L, Martinez-Orgado JA, Benito C, Millan A, Tolon RM, Romero J (2011). Cannabidiol reduces lipopolysaccharide-induced vascular changes and inflammation in the mouse brain: an intravital microscopy study. J Neuroinflammation 8: 5.

Sarnataro D, Grimaldi C, Pisanti S, Gazzerro P, Laezza C, Zurzolo C *et al*. (2005). Plasma membrane and lysosomal localization of CB1 cannabinoid receptor are dependent on lipid rafts and regulated by anandamide in human breast cancer cells. FEBS Lett 579: 6343–6349.

Sarnataro D, Pisanti S, Santoro A, Gazzerro P, Malfitano AM, Laezza C *et al*. (2006). The cannabinoid CB1 receptor antagonist rimonabant (SR141716) inhibits human breast cancer cell proliferation through a lipid raft-mediated mechanism. Mol Pharmacol 70: 1298–1306.

Sharma DK, Choudhury A, Singh RD, Wheatley CL, Marks DL, Pagano RE (2003). Glycosphingolipids internalized via caveolar-related endocytosis rapidly merge with the clathrin pathway in early endosomes and form microdomains for recycling. J Biol Chem 278: 7564–7572.

Song SK, Li S, Okamoto T, Quilliam LA, Sargiacomo M, Lisanti MP (1996). Co-purification and direct interaction of Ras with caveolin, an integral membrane protein of caveolae microdomains. Detergent-free. Purification of caveolae microdomains. J Biol Chem 271: 9690–9697.

Stella N (2009). Endocannabinoid signaling in microglial cells. Neuropharmacology 56 (Suppl. 1): 244–253.

Stella N (2010). Cannabinoid and cannabinoid-like receptors in microglia, astrocytes, and astrocytomas. Glia 58: 1017–1030.

Thors L, Alajakku K, Fowler CJ (2007). The 'specific' tyrosine kinase inhibitor genistein inhibits the enzymic hydrolysis of anandamide: implications for anandamide uptake. Br J Pharmacol 150: 951–960.

Watanabe K, Kayano Y, Matsunaga T, Yamamoto I, Yoshimura H (1996). Inhibition of anandamide amidase activity in mouse brain microsomes by cannabinoids. Biol Pharm Bull 19: 1109–1111.

Wilson BS, Steinberg SL, Liederman K, Pfeiffer JR, Surviladze Z, Zhang J *et al*. (2004). Markers for detergent-resistant lipid rafts occupy distinct and dynamic domains in native membranes. Mol Biol Cell 15: 2580–2592.

Xie XQ, Chen JZ (2005). NMR structural comparison of the cytoplasmic juxtamembrane domains of G-protein-coupled CB1 and CB2 receptors in membrane mimetic dodecylphosphocholine micelles. J Biol Chem 280: 3605–3612.

Yates ML, Barker EL (2009). Organized trafficking of anandamide and related lipids. Vitam Horm 81: 25–53.

Zhai J, Strom AL, Kilty R, Venkatakrishnan P, White J, Everson WV *et al*. (2009). Proteomic characterization of lipid raft proteins in amyotrophic lateral sclerosis mouse spinal cord. FEBS J 276: 3308–3323.